IJMF, Iranian Journal of Materials Forming, Vol.5, No. 1, pp 58-70
Printed in The Islamic Republic of Iran, 2018

Numerical and Experimental Investigation of Deep Drawing Process in Square Section of Single-Layer and Two-Layer Sheets

S. Moradi Besheli[1], S. Mazdak[1*] , H. Golmakani[1], E. Sharifi[1], M. R. Sheykholeslami[2]

[1]Department of Mechanical Engineering, Faculty of Engineering, Tafresh University, Tafresh 79611-39518, Iran.
[2]Department of Mechanical Engineering, Faculty of Engineering, Arak University, Arak 38156-879, Iran.

Abstract: Deep drawing of two-layer sheets is a suitable way to achieve fabrications with a desired shape and properties in sheet metal forming technology. To avoid deep drawing defects such as thinning is the most important challenge in this process. The greatest difficulties in this process are differences in material properties and in the geometry of each layer. In this paper, numerical approach has been exploited to plan and control the two-layer sheet deep drawing process. For this purpose, the three-dimensional (3D) finite element has been used. Stainless steel (St14) and aluminum (Al1100) (Al.St. and St.Al. lay-up) were selected as materials for the twolayer sheet metal. The results of simulation have been validated with experiments. Based on numerical study, the effect of process parameters on the percentage of thinning, maximum plastic strain, rupture, required forming force and Blank Holder Force (BHF) has been studied. The same procedure has been also done on one-layer sheet metal and the differences between deep drawing of one-layer and two-layer sheets have been comprehensively investigated. The results showed that maximum thinning occurs in the upper layer of die radial region as well as in the lower layer of punch radial region. Also, the maximum equivalent plastic strain in the lower layer is more than that in the upper layer.

Keywords: Deep drawing, Two-layer sheet, Finite element method, Equivalent plastic strain, Forming Force

1. Introduction

In deep drawing process, as one of the most applicable sheet metal forming processes, a blank is drawn into a die using a special punch to produce a cup shape work piece. In this process, stress can be both compressive and tensile. Wrinkling due to compressive stress and thinning due to tensile stress are common challenges [1]. The use of new methods for sheet metal forming such as laser forming [2], incremental forming [3] or using rubber die [4] is an interesting subject in metal forming field. Besides, the recognition of the stretchability [5] and the workability [6] of sheet metal properties is important in this field.

Multilayer sheets are defined as sheets which have at least two different layers in the area adhered to each other. These products are widely used in applications with different inner and outer working conditions (e.g. corrosion, wear resistant, thermal and electrical conductivity, etc.). Therefore, different industries such as automotive, aerospace, medical instrument and electrical industries [7] can be potentially candidate for using multilayer sheets. Multilayer laminated sheet metals, compared with single layer sheet metal, have a different forming behavior. Forming behavior of these sheets depend mainly upon the combination of material and their assembly conditions.

Mamalis et al [8] in 1997 reported a simulation study of the deep drawing of square and cylindrical cups by using the explicit non-linear finite-element code DYNA-3D. They published complementary research in this subject in 1997[9]. Parsa et al. [10] in 2001 studied the numerically redrawing of

Received by the editors December 12, 2017; Revised April 16, 2018 and Accepted April 21, 2018.
*Corresponding author (s.mazdak@tafreshu.ac.ir)

laminated Aluminum–stainless-steel sheet using FEM method with regard to anisotropy using Hill48 criteria. They validated numerical results with experiments. They showed that sheet lay-out affected drawing ratio and thickness distribution. Also, they showed that in direct redrawing, the contact between stainless-steel and the punch leads to the maximum drawing ratio and in reverse redrawing, aluminum should contact the punch in order to achieve the highest drawing ratio. Browne, [11] in 2003 used Design OF Experiment method (DOE method) to determine die radius, punch radius, clearance between die and punch, friction status, punch speed and blank thickness in order to minimize the forming force and also decrease the thinning amount. Çağlar Sönmez et al. [12] in 2005 used FEM method to study deep drawing of AL-St two-layer sheets. They introduced the amount of blank holder force, friction state and sheet layout in order to produce a product without defects. Also, the results of experiments for blank holder force were compared to the results from Hil48 criteria. Saniee et al. [13] in 2008 studied the effect of the diameter of the blank, the blank holder force, frictional condition at tool-work piece interface, contact condition of two-layer sheets and the stacking sequence with certain influences, and then examined the process of deep on the drawing process in steel-brass two-layer sheets experimentally. In their results, the distribution of thickness strain as well as some failed deep drawing tests with double-layer blanks indicated that the maximum risk of fracture for one or both of the layers is around the edge radius of the punch. Morovvati et al. [7] in 2011 used numerical approach to investigate the wrinkling of circular single layer and two-layer sheet metals in deep drawing process. They obtained the minimum required blank holder force to prevent wrinkling. Wrinkling turns out to be the principal failure mode by decreasing BHF. Results showed that the optimum blank holder force for two-layer sheets is affected by the material and arrangements of sheet lay-ups. Jalali Aghchai et al. [14] in 2008 used M-K model to study the formability of two-layer (Al1100–St12) sheets. The results showed a good agreement between theoretical and experimental results. It also showed that the formability limit of the two-layer metallic sheet is better than the lower formability of each of its components. Raju S et al. [15] in 2010 studied the impact of parameters of deep drawing in aluminum sheet 6061. Using TAGUCHI's signal-to-noise ratio, it is determined that the die shoulder radius followed by Blank Holder Force and punch nose radius has a major influence on the thickness distribution of the AA 6061 sheet deep drawn cup. Li H et al. [16] in 2013 studied deep drawing of the two-layer Steel-Steel sheet numerically and experimentally. In this research, adhesive bond between each layer was considered as a viscoelastic region. They also reported a relation between blank holder force and bonded viscosity on thickness distribution. They concluded that wrinkling exerts the main effect on lamination. Atrian et al. [17] in 2013 used FEM and experimental method simultaneously to determine important parameters such as the stacking sequence of the layers, lubrication, blank-holder force and the diameter of the composite blank on the load–displacement curve and the final shape of the produced components in the deep drawn cup of steel-brass two-layer sheet. The results of this study suggest that the permutation layers play an important role in the process of deep drawing. Safdarian et.al [18] in 2016 presented a model to predict the formability of Tailor Welded Blank sheet (TWB sheet). This model is based on limit strength ratio and thickness ratio criteria. Weld line movement and formability can be predicted with this model. Dailami et.al [19] in 2017 presented a model for the formability of two-layer sheets. This model is based on Marcinak-Kuczynski method considering non quadratic Hill failure criteria. By using this model, the formability of Al3105-St1 sheets was precisely predicted.

Mahmoodi et.al [20] in 2017 studied deep drawing of two-layer sheets, numerically and experimentally. They used Alunminum (Al1100) and Steel (St14) as work pieces. Besides, they presented a statistical model based on Taguchi method. In this model, minimum thickness was selected as the input parameter. Therefore, there was not major focus on thinning and rapture criteria. In this paper, thickness distribution in the work piece has been considered. Therefore, because of considering thickness

distribution in two critical paths, precise prediction for thinning effect and the location of thinning could be done.

In this paper, numerical and experimental methods have been used to study deep drawing of two-layer and single layer sheets in square section by numerical method that has been investigated. Since the square cups have rounded corners and straight walls, the drawing behavior and wall thickness distribution in the corners of the cup is a challenge. Also, the existence of different properties in each layer causes defects such as thinning, rupture and wrinkling in the produced pieces. The use of rectangular shape with a two-layer sheet creates different conditions compared to previous surveys providing grounds for reviewing this aspect. The results of numerical study have been validated with experimental test. In the numerical study, minimum BHF to prevent the initiation of wrinkling, required forming force, and maximum plastic strain were calculated via finite element simulation. ST14 and Al1100 sheets were selected as materials for experimental validation. These materials have been tested individually and in combination as a two-layer sheet. The effect of material and lay-up on appropriate BHF, forming forces, and plastic strain has been presented based on the numerical and experimental studies. Deep drawing parameters were the same in the single layer and two-layer deep drawing. Also, in this paper, a comprehensive comparison between the main parameters in deep drawing of one-layer and two-layer sheets has been presented.

2. Material and Method

2.1. Properties of materials

Tensile test according to ASTM (E8) has been done on Al 1100 steel St14 sheets with a thickness of 0.7 mm. The mechanical properties of ST14 and aluminum 1100 were derived from tensile test, and they have been listed in Table 1.

Table 1. mechanical properties of materials.

Sheet material	Young's modulus (E GPa)	Poisson 's ratio(ν)	Density (kg/m^3)	Yield Stress (MPa)	Strength coefficient (MPa)	Strain Hardening (n)
Aluminum 1100	70	0.33	2560	79.57	160.7	0.149
Steel ST14	200	0.29	7800	180.33	385.8	0.23
Polyurethane	90	0.29	1300	43	-	-

The thicknesses of ST14 and Al1100 sheets were the same (1.4 mm), and the two-layer sheet was made of 0.7 mm ST14 and 0.7 mm Al1100 sheets. In experiments, blanks with the 80 mm diameter were used and punch with 5 mm/s axial movement speed formed the blanks. Blank holder was used during the process. Different lay-ups that were investigated in this paper have been predicted in Fig.1. The layers were bonded together by glue. Polyurethane adhesive with the presented properties is shown in (Table 1). The stress–strain curve for this material has been shown in Fig. 2. This graph has been experimentally derived from tensile test.

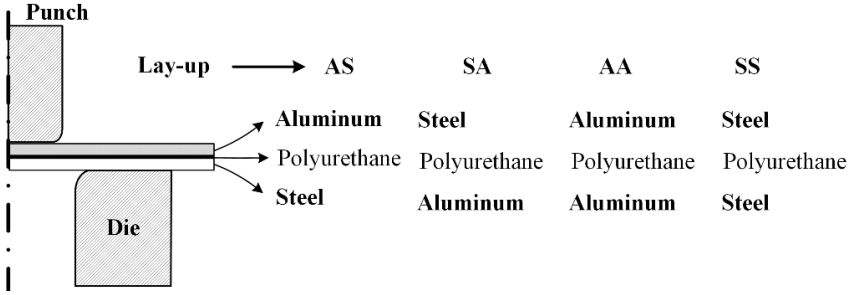

Fig 1. Different lay-ups that have been used.

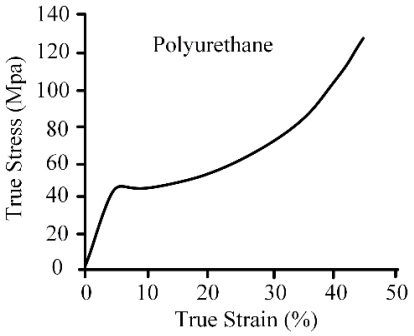

Fig. 2. True stress strain curve of polyurethane.

2.2. Numerical study

2.2.1. Modeling

By using finite element simulation, the effect of required BHF and forming force on the wrinkling and fracture and maximum equivalent plastic strain of single layer and two-layer sheets has been studied. ABAQUS/CAE 6.13 Explicit/FEM code has been selected as commercial software in finite element simulation. Geometrical model for finite element simulation is shown in Fig. 3. Due to the symmetry in the geometry of the sample, a quarter of the model has been analyzed. All parts of the die including punch, blank holder and the die are assumed a rigid body in the simulation. The blank has been considered as a shell. Rigid surfaces should be half the thickness of the shell from each other's distance.

2.2.2. Boundary condition

Symmetric boundary condition existed in the numerical study. All degrees of freedom for the blank holder and die were fixed and the displacement amount of punch was 10 mm. Symmetrical constraint was applied on the edges of the sheet. The contact between the die and blanks was modeled by surface to surface interaction. The middle layer was bonded tightly with the internal and external layers. Materials were used in the power hardening law and isotropic for each layer. Because the middle layer, polyurethane, was extremely thin and it was assumed that the alignment of the middle layer would not affect the forming process, tie limit was used to create cohesion between two-layer sheets in all points. Also, the friction coefficient was selected 0.1, according to the literature survey [15].

2.2.3. Meshing

Mesh in all elements of this simulated model was quad and the structured technique was used to generate meshes. The analysis has been done dynamically explicit. The condition of analysis and mesh has been applied in a way that the kinematic energy is less than 10% of the total energy. Independency from the mesh size has been considered in simulation. Table 2 shows meshing properties in this simulation.

Table 2. Type of element and properties of simulated die.

Type of part	Type	Element	
Punch	Rigid	R3D4	4-node, 3D
Blank holder	Rigid	R3D4	4-node, 3D
Sheet	Deformable	S4R	4-node, 3D reduced integration
Die	Rigid	R3D4	4-node, 3D

Thickness distribution has been determined in two paths of A and B, which is shown in Fig. 4. Thinning diagrams have been obtained by measuring in 14 points of the produced part in experimental method and also in the simulation. The measured points were placed in five points of different sections in the produced parts. Figure 4 shows the paths and the determined area in the produced part.

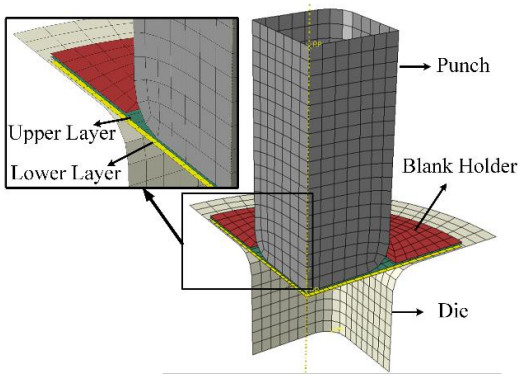

Fig. 3. 3D geometrical model for finite element simulation.

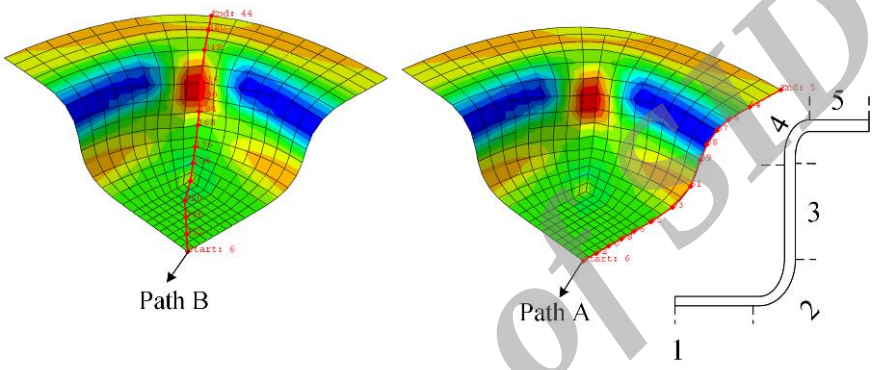

Fig. 4. Designated paths in samples of simulation and divided regions in the produced part.

3.2. Experimental setup

A die with constant blank holder force has been designed in order to perform the experimental tests. The experimental setup has been shown in Fig. 5. Deep drawing die consisted of two upper and lower parts. The upper part included the upper hoof which was connected to the movable part of the press. Also, drawing punch, punch stuck, fixed ring, holder ring, blank holder and two bearings were connected to this hoof. The lower part included the lower hoof, drawing die and two guide bars which were held on the fixed part of the press. The blank holder force to control the sheet flow was supplied by four springs, and it created a 2000 N of BHF. In addition, the fixed ring was held by four springs which created a 12000 N of force. Table 3 shows the dimensions of the die and the two-layer sheet.

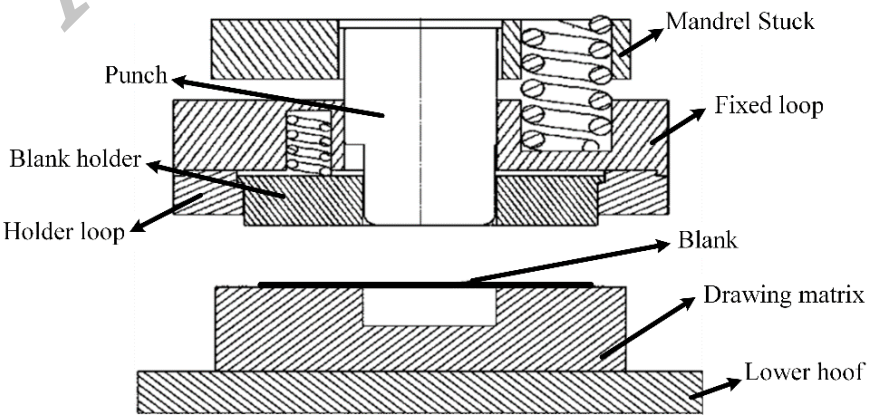

Fig. 5. Designed die of deep drawing process.

Table 3. Dimensions of made die.

Parameter	Dimension (mm)
Sheet holder cavity	44 × 44
Radius of the corner of the die and the punch	5
Die cavity	43.08 × 43.08
Punch	40 × 40

Determining the placement speed of the punch and blank holder force as well as the affecting parameters in the process is important. Suitable considerations have been applied on the experimental setup. Fig.6 shows the mounted die on the press.

Fig. 6. Deep drawing die used in experiments.

Figures 7 and 8 show the produced parts by single layer and two-layer sheets in a practical work. The single layer sheet included aluminum 1100 and steel ST14. The two-layer sheet included AS, SA, AA, SS.

Fig. 7. Single layer cups. (a) Aluminum 1100, (b) Steel ST14.

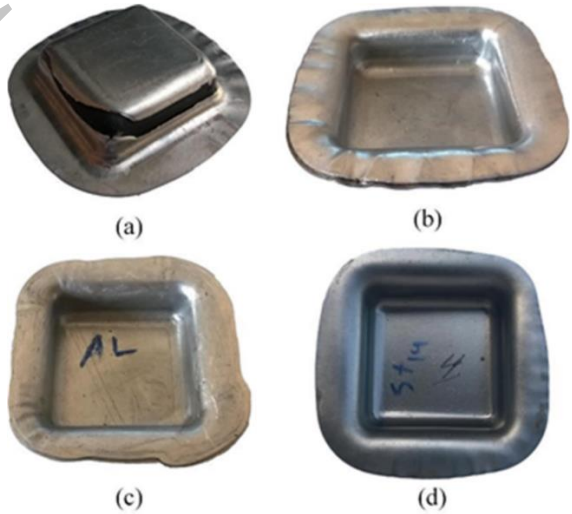

Fig. 8. Two layer cups (a) AS sheet, (b) SA sheet, (c) AA sheet, (d) SS sheet.

A micrometer has been used to measure the initial thickness of the blank. All the parts were cut in two paths of A and B and the thickness in a specified direction to determine the thickness (t) distribution by measuring the gauges. At last, the average of thickness for these points were determined. Figure 9 shows the cut line in the parts to determine the thickness distribution.

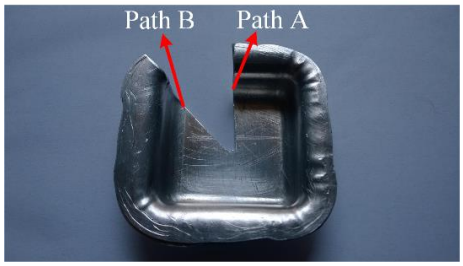

Fig. 9. Designated paths in parts produced.

3.4. FEM validation

Figure 10 shows the thickness distribution of the cup in a single-layer of aluminum and steel based on FEM simulation. The difference in the drawing behavior in paths A and B arose from different distribution of thickness along these paths. The maximum thinning in the steel single-layer was in path B and in punch radius which was 28.34% more than the highest percent of thinning in aluminum single-layer. Rupture has not occurred in the steel layer due to high strength compared to aluminum layer. Also, the steel layer had maximum thickening along path B in the die radius profile (region 4), compared to other investigations.

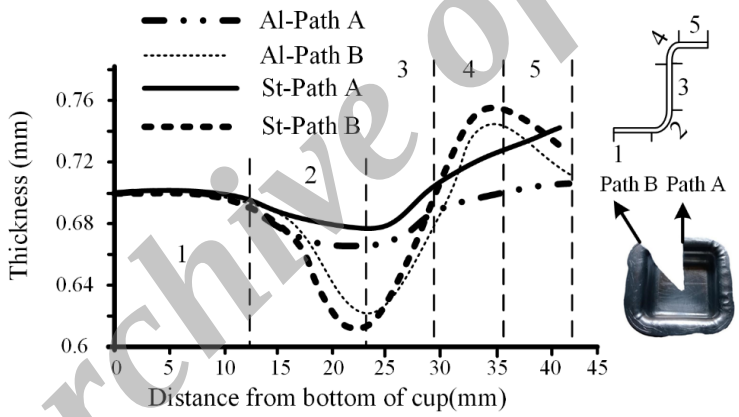

Fig. 10. Thickness distribution in single-layer aluminum and steel based on simulation.

Figure 11 shows the thickness distribution in the aluminum layer and two-layer sheets based on permutation (Lay-up) in the experiment and also in the simulation in path B. During the whole survey, the aluminum layer in the corner wall of the cup had the maximum thinning (region 2). This thinning was more when the aluminum sheet was in the lower layer of AS sheet. Due to the rupture in the aluminum layer of AS sheet (Fig 8a), the highest percent of thinning in this layer, in the experiment, in the corner wall of the cup was 4.65% more than the numerical analysis in two-layer of AS. Besides, the minimum thinning in this region occurred while the aluminum sheet was considered as the upper layer of SA and the rupture in this layer was prevented (Fig 8b). The results showed that the maximum thinning in the lower layer of AS was 86.26% more than that of the upper layer of SA sheet. In addition, it is clear that the aluminum single-layer was thinning because it was used as the lower layer in the two-layer sheet and thinning had been reduced when it was used as an upper layer of the two-layer sheet. Also, this figure showed the percentage of difference in the thickness for the experimental and numerical results in the corner wall of the cup for the lower layer of AS.

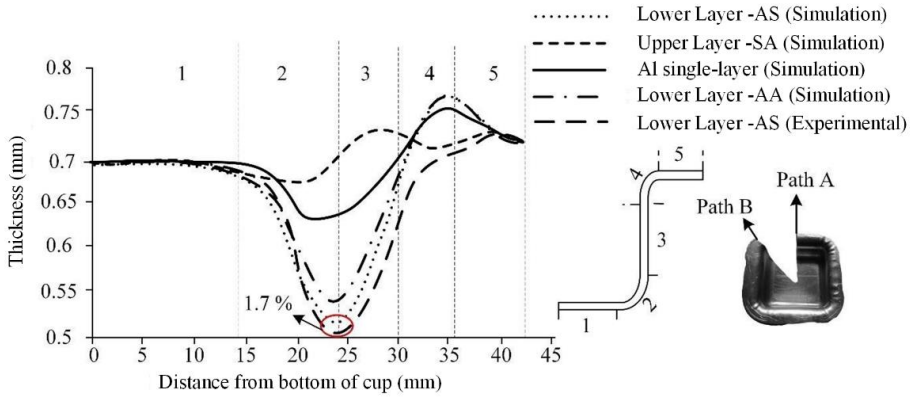

Fig. 11. Thickness distribution of aluminum single-layer and two layer sheets based on layup in path B.

Figure 12 shows the thickness distribution in steel single-layer sheet and two-layer sheet based on lay-up in practice and the simulation in path B. This figure shows that thinning was more in the corner wall of the cup (punch radius). Thinning increased in this region while the steel layer was in the lower layer of SS sheet. The highest percent of thinning from numerical simulation in the lower layer of SS layer was 18% more than that in the experimental work.

Despite considerable thinning of the layer, the rupture did not occur because of high strength in the steel layer (Fig. 8d). The highest percentage of thinning in the lower layer of SS sheet was 60.81 percent more than that of the state where the steel layer was in the upper layer of AS sheet. This result shows the effect of permutations layers on thinning effect. Also, the percent of thinning in a single-layer steel (in the upper layer) and a two-layer (in the lower layer) one decreased and increased respectively.

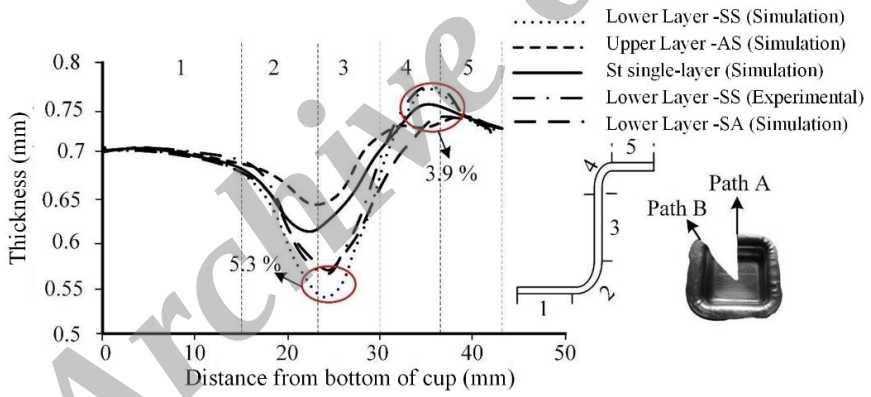

Fig. 12. Thickness distribution of steel single-layer and two-layer sheets based on lay-up in path B.

4. Results and Discussion

4.1. Blank holder force

Figure 13 shows the punch displacement versus the blank holder force for different materials in single and two-layer sheets. Proper BHF is one of the most important and effective factors in successful drawing operations. Performing several examinations is necessary to determine the minimum BHF to avoid wrinkling in specific conditions. In other reports, several deep drawing tests with different BHFs were carried out to determine a minimum BHF value that prevented wrinkling. Using higher BHF causes fracture during the deep drawing process. In this study, during the simulation the blank holder at a distance was identified based on the two-layer or single layer sheets; thickness was kept constant and then the reaction force (required BHF) was measured. This procedure was done for each of ST14, Al 1100, ST14-Al1100 (AS) and Al1100-ST14 (SA) sheets. This procedure has reduced the number of numerical simulations for determining a suitable BHF. The required BHF for the two-layer sheet SS was 13550 N. It is shown in region 1 in (Fig. 13). The required BHFs for AS, SA, steel single layer and aluminum single

layer sheets were 8334 N, 8577 N, 9800 N and 2930 N, respectively. According to the results, the SS two-layer sheet needs more BHF than the other one. Based on the numerical simulation, a lower value can cause wrinkling, and a higher value leads to the prevention of wrinkling in addition to increasing the probability of rupture due to a lack of appropriate flow sheet. It can be concluded that the sheet with higher strength required more BHF according to Fig. 13. In other words, less BHF can be used for a sheet with higher ductility to control its wrinkling. Based on the results, it can be seen that the required BHF for a two-layer sheet is between the required BHFs for 2 constructing layers. It means that the required BHF for a two-layer sheet depends on the characteristics of its components and is less than the BHF for the stronger sheet and more than the BHF of the weaker one. It was the applicable and also the interesting point in planning the deep drawing process. Furthermore, for two-layer sheets, it has been observed that the required BHF for SA (A.I. lay-up) was more than the BHF for AS (S.I. lay-up). This can be related to the higher value of the induced tension in the flange area for this lay-up. Consequently, the value of the required BHF is the highest for SA (A.I. lay-up).

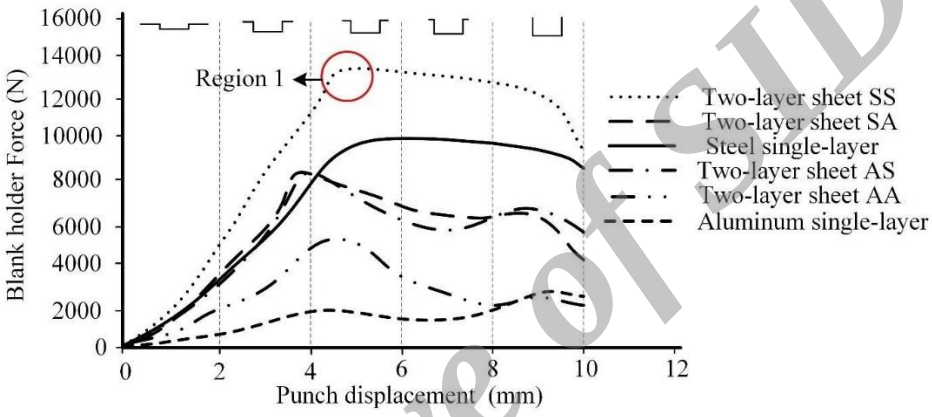

Fig. 13. Blank holder versus force- punch displacement curve for single and two-layer sheets.

4.2. Reshaping force

Figure 14 shows the relationship between the punch load versus the punch displacement- based on one-layer and two-layer sheets. Regarding this figure, the reshaping force for ST14– Al1100 (A.I. and S.I. lay-up) was higher than that of aluminum and lower than that of steel. That was why it happened; the resultant yield stress of the two-layer sheet was a function of its components' yield stress. In other words, the mechanical properties of the two-layer sheet depend on its components and they are more than the weaker sheet and less than the stronger one. The decrease in the forming force for the S.I. lay-up is due to two main reasons. First, the frictional stress between the die and the sheet was less for aluminum sheet in comparison to the steel sheet that decreased the forming forces. Second, the resultant bending and unbending load is less for the S. I. lay-up due to the increase of the bending radius. The maximum load was applied for reshaping the two-layer sheet SS. The maximum forming force for this two-layer sheet was 28 and 32% more than SA and AS two-layer sheets respectively.

The numerical analysis of the equivalent plastic strain in deep drawing process was done to obtain the metal flow law of the drawn part. Figure 15 shows the influences of yield stress σ_y and also the lay-up on the equivalent plastic strain (PEEQ) along the path B of the drawn surface part in the single layer Al 1100, ST14 and ST14– Al1100 (A.I. and S.I. lay-up). It can be seen that when σ_y increased (steel layer), the maximum equivalent plastic strain would occur near the wall region outside the die radius (region 4), because this area was potentially a dangerous location for a crack. Wrinkle was observed at this region and also in the flange portion of the part. When the yield stress decreased (aluminum layer), the equivalent plastic strain would increase suddenly near the punch radius (region 2), indicating that tearing of the

material took place. It was clear that the permutation of a single layer in two-layer sheets changed the maximum of PEEQ. According to the results of the presented study, the maximum equivalent plastic strain based on material occurs in a single layer (aluminum or steel). Also, the maximum equivalent plastic strain in the lower layer of the two-layer sheet was more than that in the upper layer. As previously mentioned, the lower layer has more stretching strain than the upper layer. That is why the risk of rupture is greater in this layer. The maximum of PEEQ in aluminum layer of AS sheet was 39% more than that of the aluminum layer of the SA sheet. Also, the maximum of PEEQ in the steel layer of the SA sheet was 16% more than that of the steel layer of AS sheet.

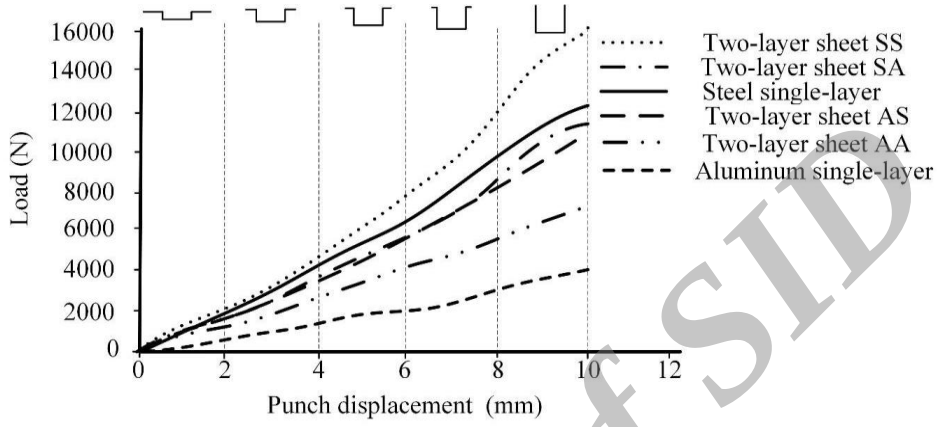

Fig. 14. Reshaping force versus punch displacement for single and two-layer sheets (Simulation).

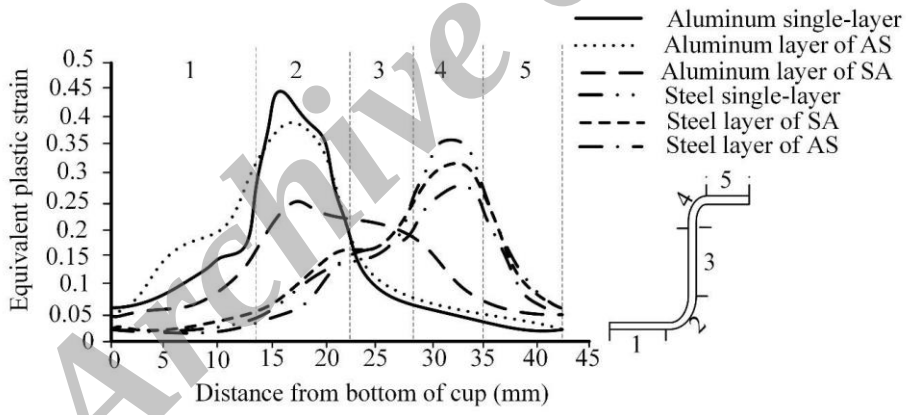

Fig. 15. Equivalent plastic strain distribution in single and two layer sheets.

5. Conclusion

In this paper, the numerical simulation and experimental validation of deep drawing process in the single-layer and two-layer sheets (Aluminum and steel sheet individually) and their combination have been done. Also, the effect of parameters such as the percentage of thinning, maximum strain of plastic, rupture, maximum forming force and required blank holder force have been studied. Based on the results of this paper:

1. In a two-layer sheet, when the aluminum layer is in the lower layer of the AS sheet, thinning is higher than the other alternative in single layer and two-layer sheets based upon Aluminum and Steel. The maximum thinning in the lower layer of the AS was 86.26% more than that in the upper layer of SA sheet. In addition, it is clear that aluminum and steel single-layer sheets were thinning because they were used as the lower layer in two-layer sheets.

2. Layer stacking sequence played a significant role in this process. By changing the layer sequence, different properties are obtained for the product.
3. The higher the strength of sheet material, the more the required BHF to eliminate its wrinkling during the deep drawing process. Also, less BHF can be used for a sheet with higher ductility to control its wrinkling.
4. The required BHF and forming force for a two-layer sheet depends on the characteristics of its components and are less than the values of the stronger sheet and more than the values of the weaker one.
5. The required BHF and forming force for Al-St lay-up are 2.83% and 5% higher than the values for the St-Al lay-ups, respectively.
6. When σ_y increases (steel layer), the maximum equivalent plastic strain occurs near the wall region outside the die radius (region 4) and when the yield stress decreases (aluminum layer), the equivalent plastic strain increases suddenly near the punch radius (region 2). Also, the maximum equivalent plastic strain in the lower layer is more than that of the upper layer.

References

[1] F. W. Hosford, R. M. Caddell, Metal forming: mechanics and metallurgy, Cambridge University Press, (2011) 225-228.

[2] M. Safari, M. Farzin, H. Mostaan, A novel method for laser forming of two-step bending of a dome shaped part, *Iranian Journal of Materials Forming* 4(2) (2017) 1-14.

[3] M. Safari, Two Point Incremental Forming of a Complicated Shape with Negative and Positive Dies, *Iranian Journal of Materials Forming* 4(2) (201751-61.

[4] M. Sheykholeslami, S. Cinquemani, S. Mazdak, Numerical study of the of ultrasonic vibration in deep drawing process of circular sections with rubber die. In Active and Passive Smart Structures and Integrated Systems XII, *International Society for Optics and Photonics* 10595 (2018) 539.

[5] S. Kathiravan, A. N. Sait, M. Ravichandran, Experimental Investigation on Stretchability of an Austentic Stainless Steel 316L, *Iranian Journal of Materials Forming* 3(1) (2016) 55-64.

[6] H. Vafaeenezhad, S.H. Seyedein, M.R. Aboutalebi, A. R. Eivani, Workability Study in Near-Peritectic Sn-5% Sb Lead-Free Solder Alloy Processed by Severe Plastic Deformation, *Iranian Journal of Materials Forming* 3(2) (2016) 39-51

[7] M.R. Morovvati, A. Fatemi, M. Sadighi, Experimental and finite element investigation on wrinkling of circular single layer and two-layer sheet metals in deep drawing process, *The International Journal of Advanced Manufacturing Technology* 54(1) (2011) 113-121.

[8] A. G. Mamalis, D. E. Manolakos, A. K. Baldoukas, Simulation of sheet metal forming using explicit finite-element techniques: effect of material and forming characteristics: part 1. Deep-drawing of cylindrical cups, *Journal of materials processing technology* 72(1) (1997) 48-60.

[9] A. G. Mamalis, D. E. Manolakos, A. K. Baldoukas, Simulation of sheet metal forming using explicit finite element techniques: effect of material and forming characteristics: Part 2. Deep-drawing of square cups, *Journal of Materials processing technology* 72(1) (1997) 110-116.

[10] P. Mohammad Habibi, K. Yamaguchi, N. Takakura, Redrawing analysis of aluminum–stainless-steel laminated sheet using FEM simulations and experiments, *International journal of mechanical sciences* 43(10) (2001) 2331-2347.

[11] M. T. Browne, M. T. Hillary, Optimizing the variables when deep-drawing CR 1 cups, *Journal of materials processing technology* 136(1) (2003) 64-71.

[12] S. Çağlar, A. Erman Tekkaya, C. Hakan Gür, Comparison of the deep drawability of aluminum and steel using numerical simulation experiments, *AIP Conference Proceedings* 778(1) AIP (2005).

[13] F. Fereshteh-Saniee, A. Alavi-Nia, A. Atrian-Afyani, An experimental investigation on the deep drawing process of steel–brass bimetal sheets. *Proceedings of metal forming. Krakow, Poland, Conference, Conference*. (2008) 63-70

[14] Aghchai, A. Jalali, M. Shakeri, B. Mollaei-Dariani, Theoretical and experimental formability study of two-layer metallic sheet (Al1100/St12), *Proceedings of the Institution of Mechanical Engineers*, Part B: *Journal of Engineering Manufacture* 222(9) (2008) 1131-1138.

[15] S. Raju, G. Ganesan, R. Karthikeyan, Influence of variables in deep drawing of AA 6061 sheet, *Transactions of Nonferrous Metals Society of China* 20(10) (2010) 1856-1862.

[16] H. Li, J. Chen, J. Yang, Experiment and numerical simulation on delamination during the laminated steel sheet forming processes, *International Journal of Advanced Manufacturing Technology* 68 (2013).

[17] A. Atrian, F. Fereshteh-Saniee, Deep drawing process of steel/brass laminated sheets, *Composites Part B: Engineering* 47 (2013) 75-81.

[18] R. Safdarian, M.J. Torkamany, A Novel Approach for Formability Prediction of Tailor Welded Blank, *Iranian Journal of Materials Forming* 3(2) (2016) 1-12

[19] H. Deilami Azodi, R. Darabi, A Comparative Study on the Formability Prediction of two-layer metallic Sheets, *Iranian Journal of Materials Forming* 4(1) (2017) 39-51.

[20] M. Mahmoodi, H. Sohrabi, Using the Taguchi Method for Experimental and Numerical Investigations on the Square-Cup Deep-Drawing Process for Aluminum/Steel Laminated Sheets, *Mechanics of Advanced Composite Structures* 4(2) (2017) 169-177.

بررسی عددی و تجربی فرآیند کشش عمیق مقطع مربعی ورق‌های تک لایه و دولایه

سامان مرادی بشلی[1]، سیامک مزدک[1]، حمید گلمکانی[1]، ابراهیم شریفی[1]،
محمد رضا شیخ الاسلامی[2]
[1]دانشکده فنی و مهندسی، گروه مکانیک، دانشگاه تفرش، تفرش، ایران
[2]دانشکده فنی و مهندسی، گروه مکانیک، دانشگاه اراک، اراک، ایران

چکیده: فرآیند کشش عمیق دو لایه روشی مناسب برای ساخت قطعات در شکل و خصوصیات مورد نظر در شکل‌دهی ورقی می باشد. اجتناب از عیوبی همچون نازک‌شدگی از مهمترین مسائل در این فرآیند می‌باشد. از دشواریهای این فرآیند تفاوت خصوصیات و هندسه لایه‌های بهم چسبیده می‌باشد. در این مقاله از روشهای عددی برای طراحی و کنترل ورق‌های دو لایه در فرآیند کشش عمیق استفاده شده است به این منظور شبیه‌سازی‌هایی المان محدود به‌صورت سه‌بعدی، برای دو جنس فولاد (St14) و آلومینیوم (Al1100) انجام شده است و صحت شبیه‌سازی‌ها توسط آزمایش تجربی بر اساس این مقاله، بررسی شده است. در ادامه تاثیر پارامترهایی از قبیل: حداکثر درصد نازک‌شدگی، حداکثر کرنش پلاستیک موثر، پارگی، بیشترین نیروی سنبه و ورق‌گیر(BHF) در ورق‌های تک و دولایه فولادی و آلومینیومی بررسی شده است. نتایج نشان دادند که بیشترین نازک‌شدگی در لایه بالایی، در ناحیه شعاع ماتریس و در لایه پایینی در شعاع سنبه اتفاق می‌افتد؛ همچنین بیشترین کرنش معادل پلاستیک در لایه پایینی بیشتر از بیشینه کرنش پلاستیک لایه بالایی می‌باشد.

واژه های کلیدی: کشش عمیق، ورق‌های دو لایه، المان محدود، کرنش پلاستیک، نیروی شکل‌دهی